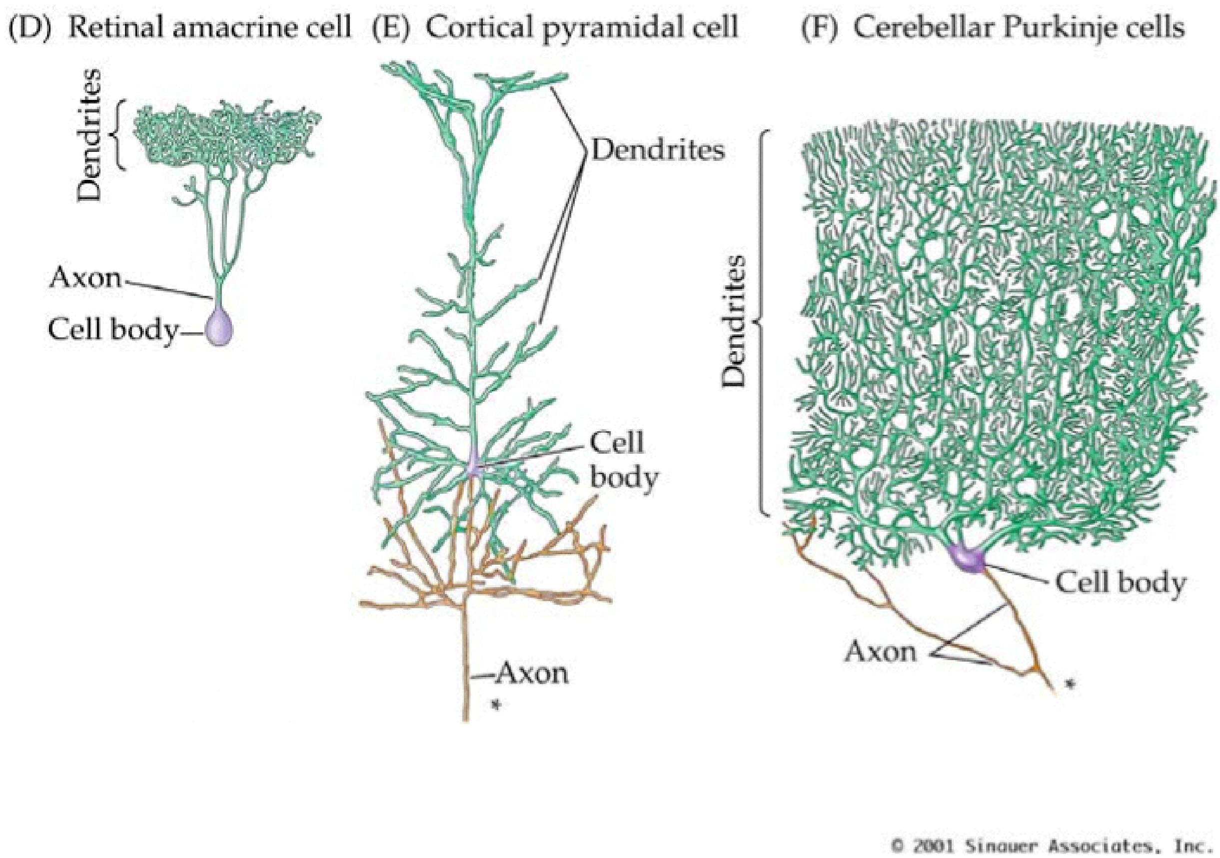

01_neurons.pdf

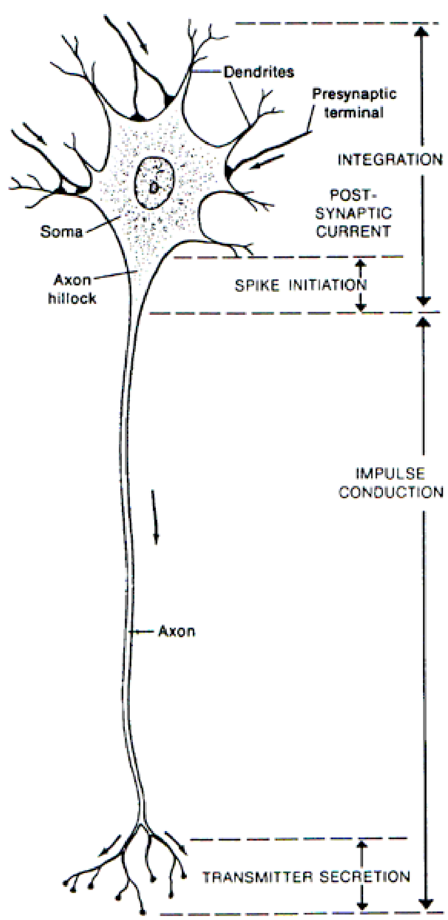

02_neuronParts.tif

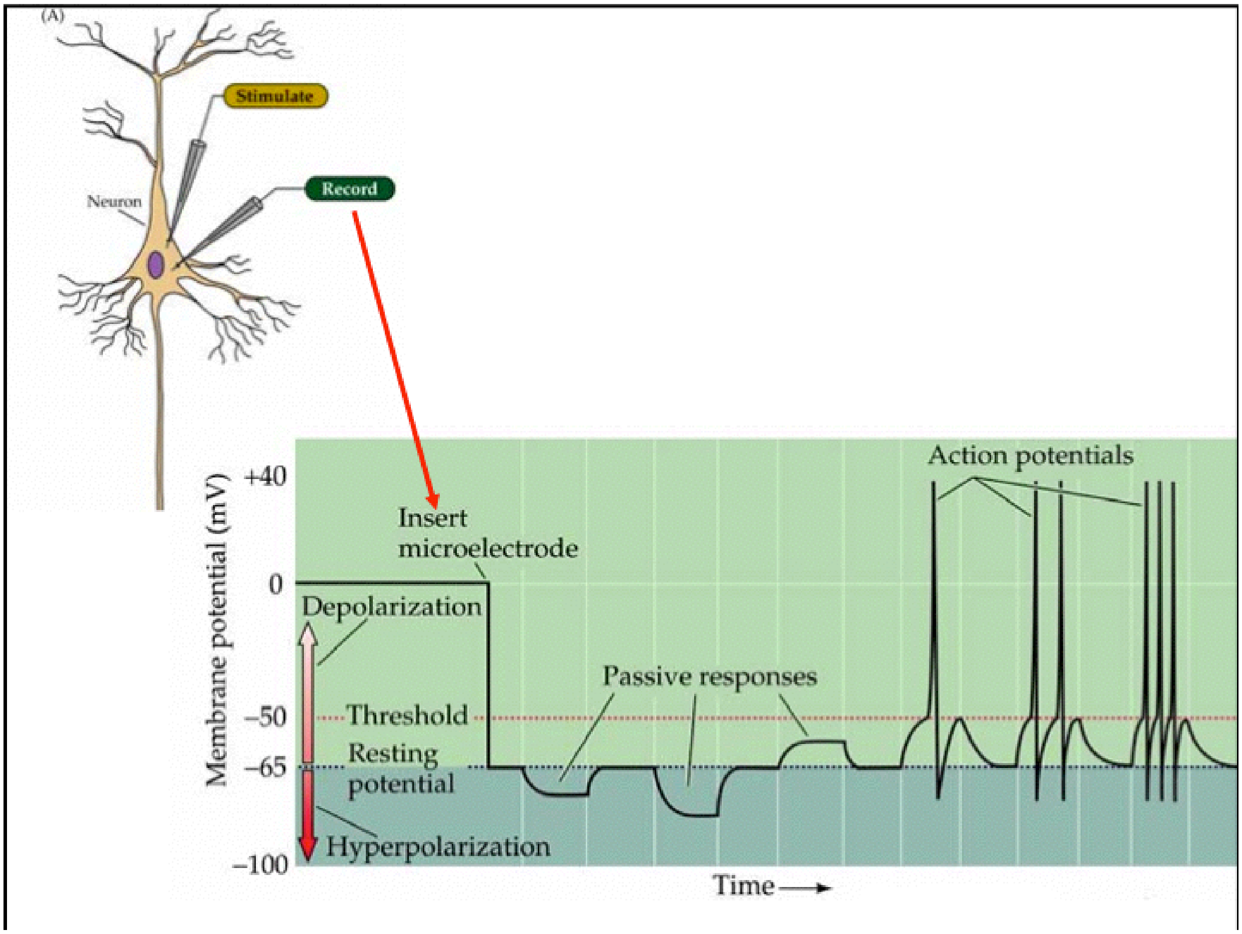

03_memPot.pdf

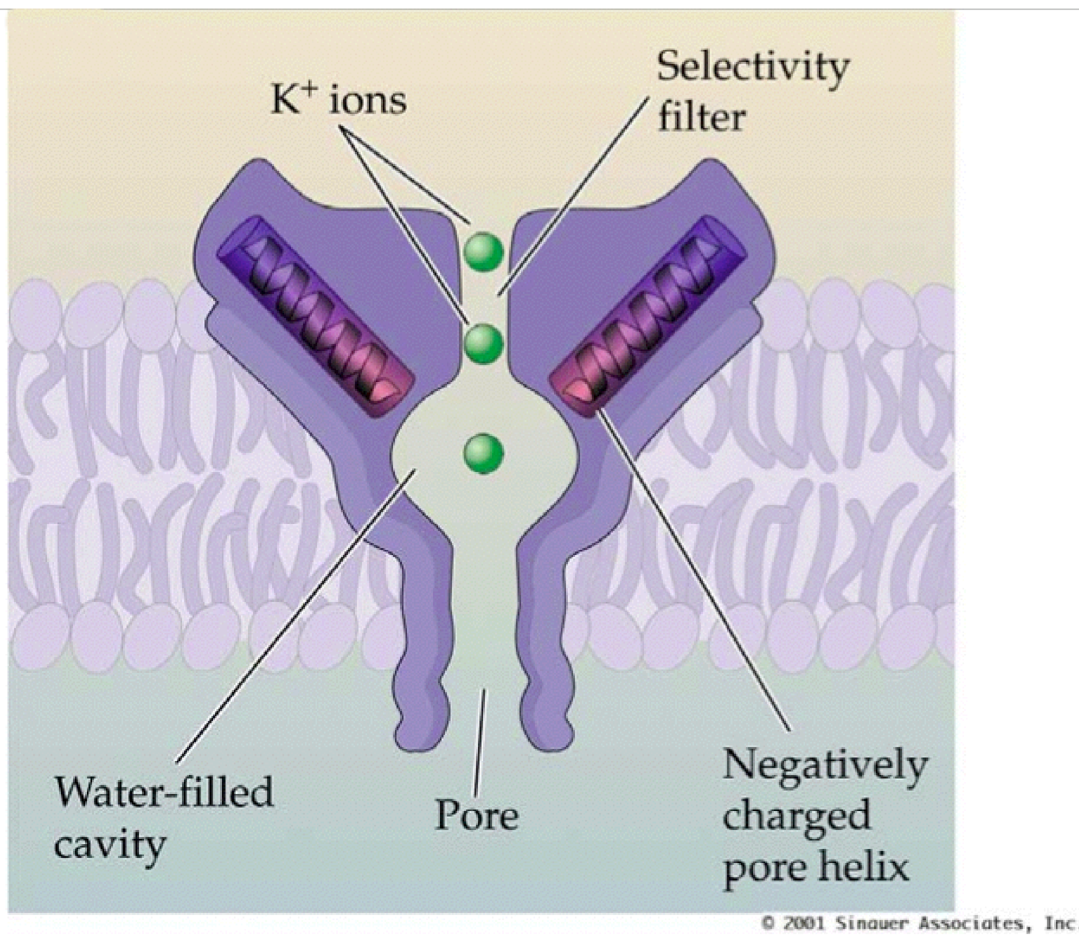

04_channel.pdf

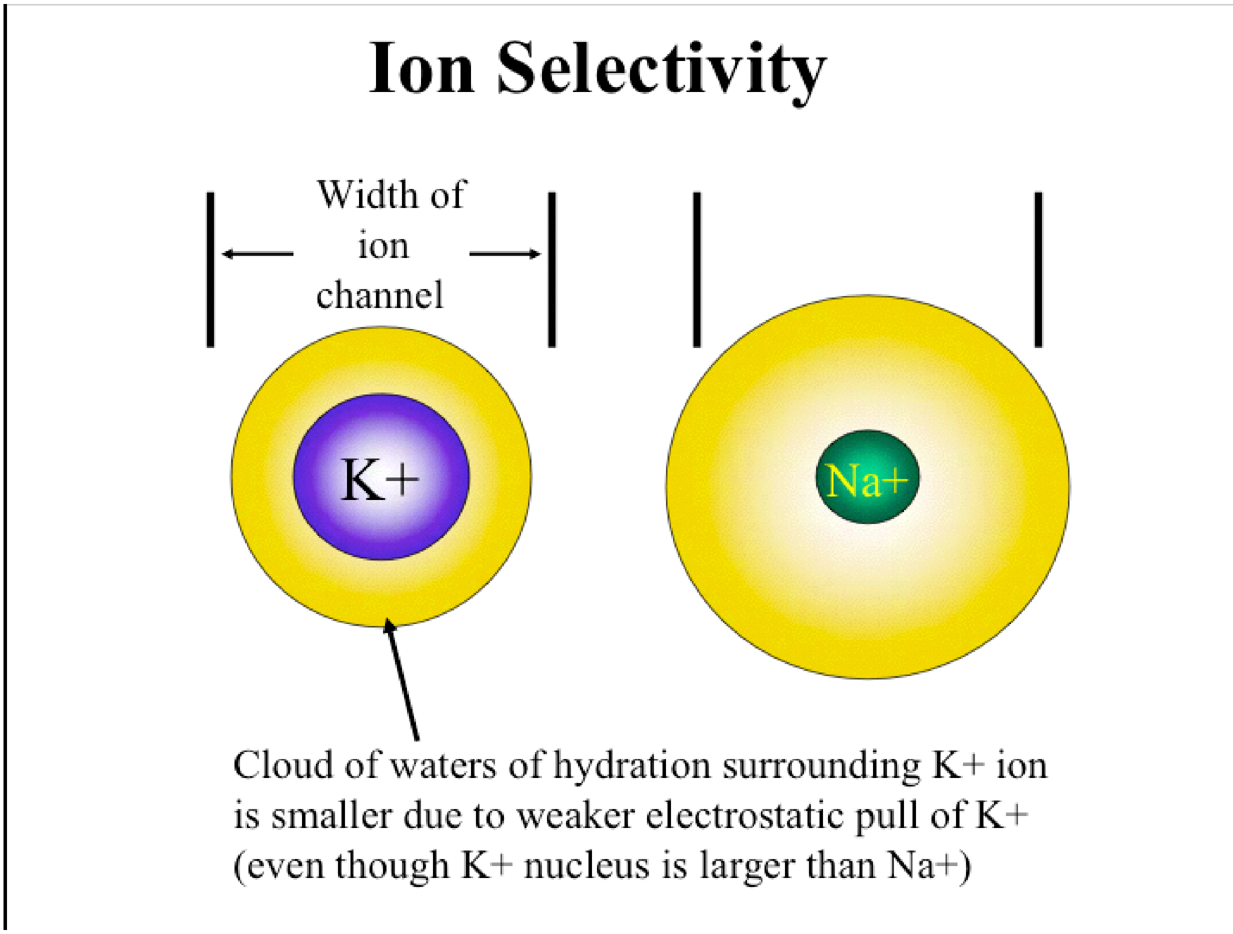

05_ions.pdf

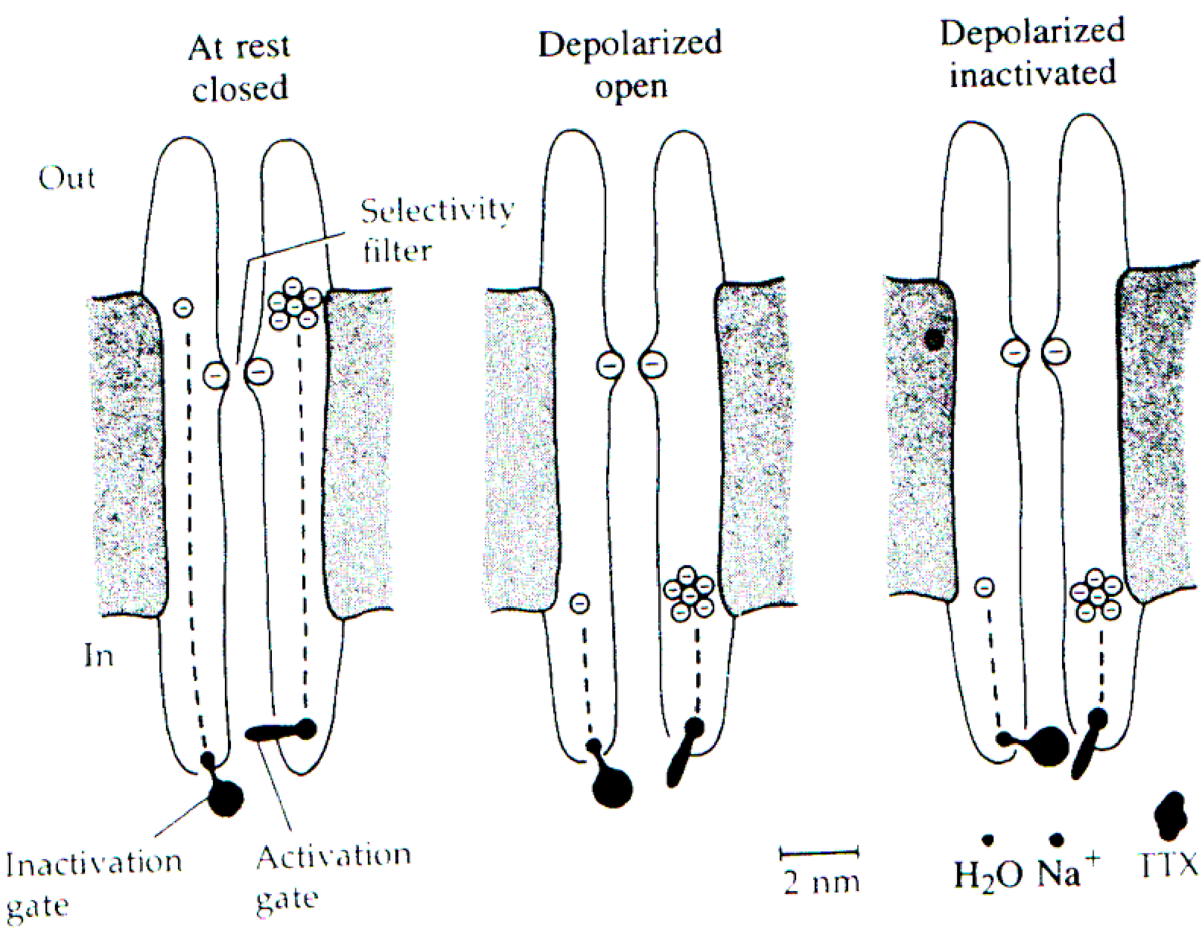

06_channelGate.tif

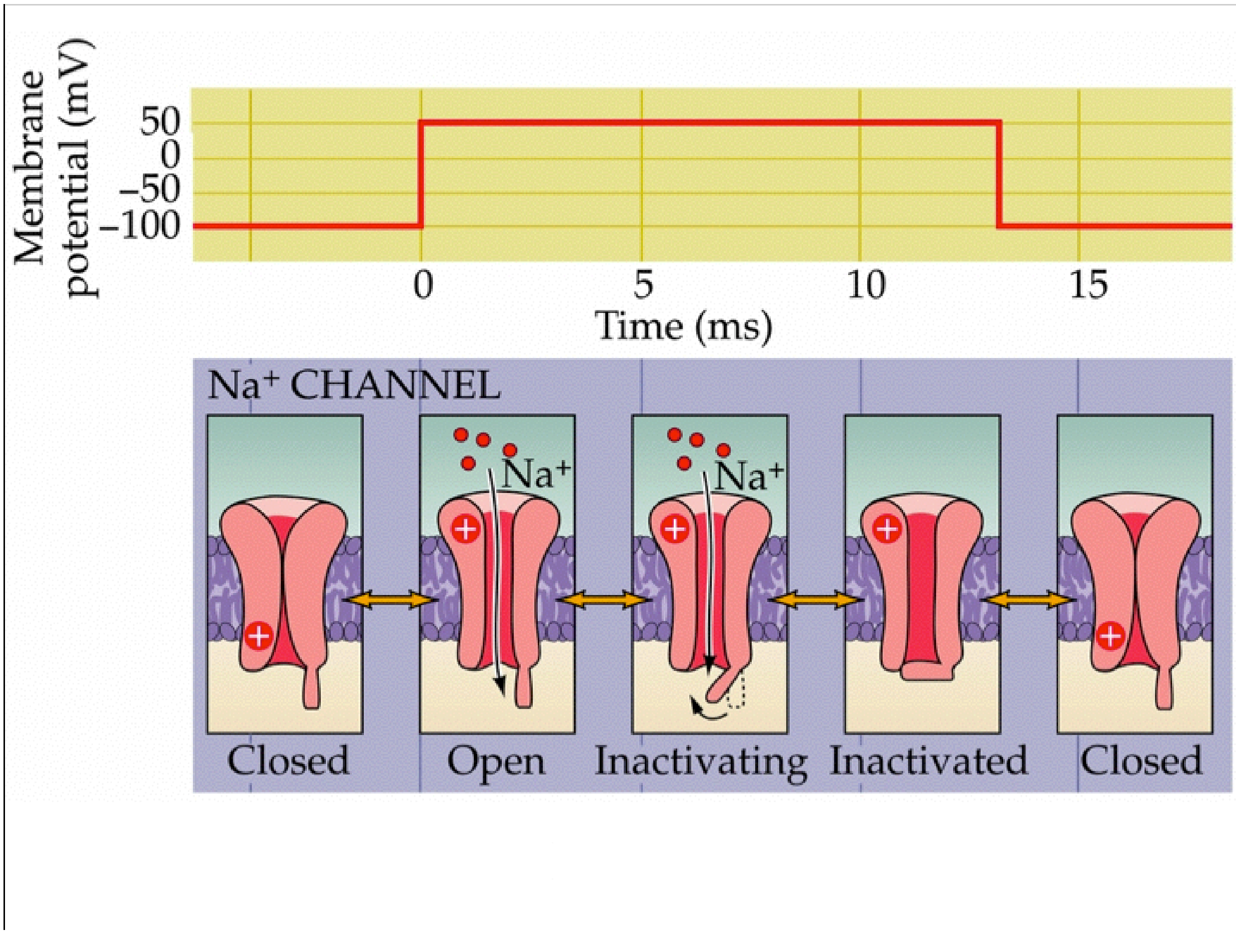

07_channelStates.pdf

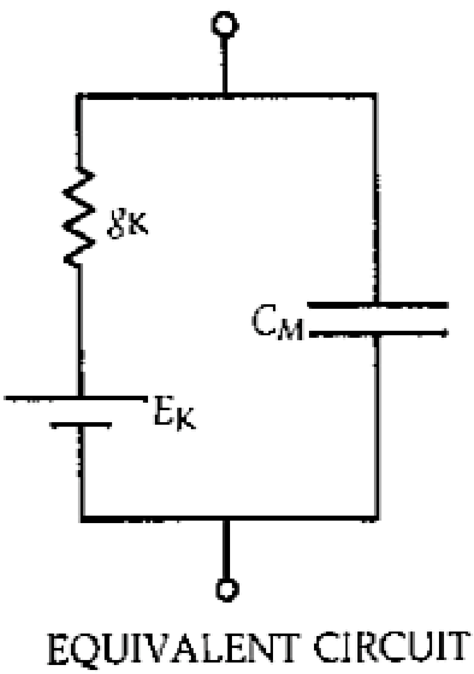

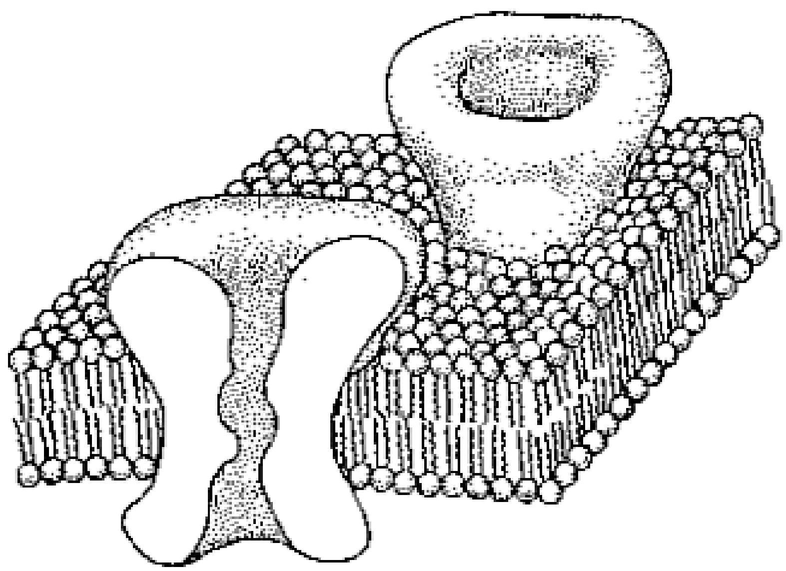

08_equivCircuit.psd

Current-Voltage Equation

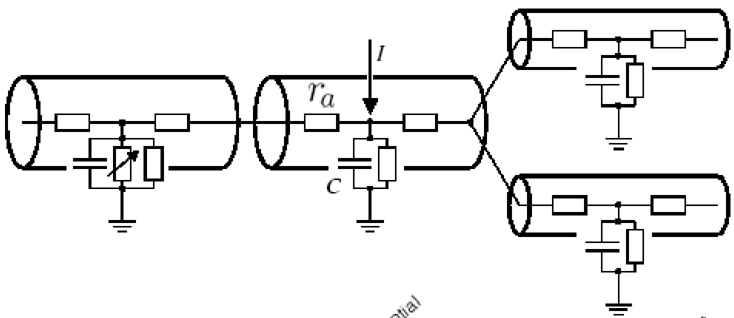

membrane potential

injected current

$$\frac{1}{r_a}\frac{\partial^2 V}{dx^2} + C\frac{dV}{dt} = I$$

09_IV_eq.psd

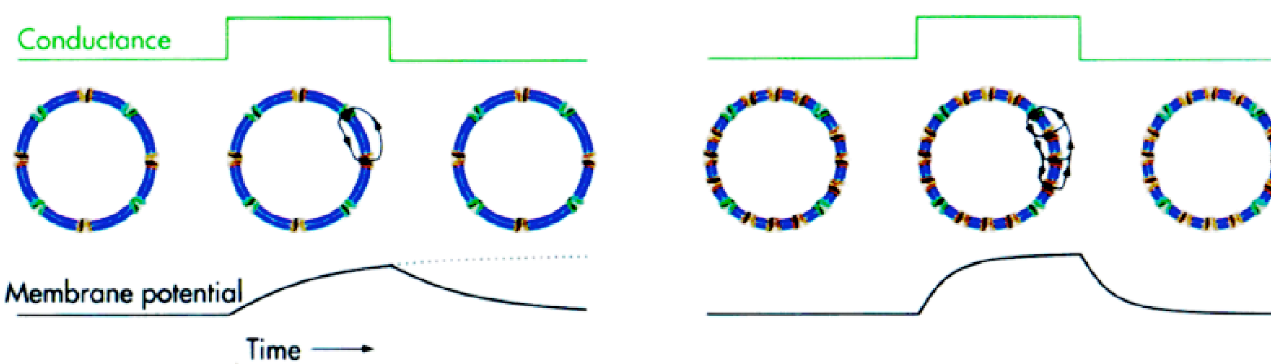

injected current

leak current

$$C\frac{dV}{dt} = I_{stim} - g_L(V - V_L)$$

The Human Brain: An Introduction to Its Functional Anatomy (1999) John Nolte

10_leakyMembrane.psd

Hodgkin-Huxley Equation

$$C\frac{dV}{dt} = I_{stim} - g_L(V - V_L) - \bar{g}_{Na}m^3h(V - V_{Na}) - \bar{g}_K n^4(V - V_K)$$

injected current, leak current, sodium current, potassium current

$$\frac{dm}{dt} = \frac{1}{\tau_m}(m_\infty(V) - m) \qquad \frac{dh}{dt} = \frac{1}{\tau_h}(h_\infty(V) - h) \qquad \frac{dn}{dt} = \frac{1}{\tau_n}(n_\infty(V) - n)$$

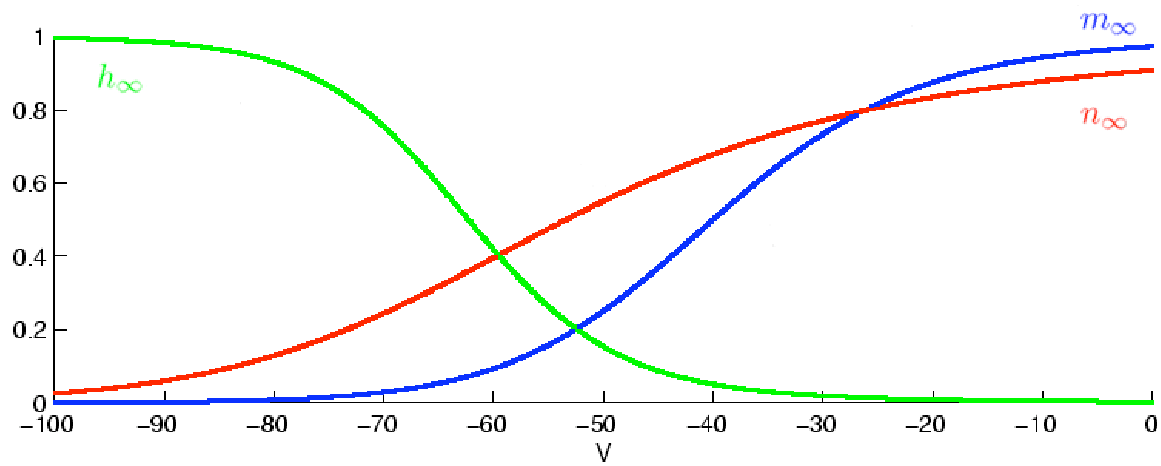

11_hh_eq.psd

Molecular Structure of Ion Channels

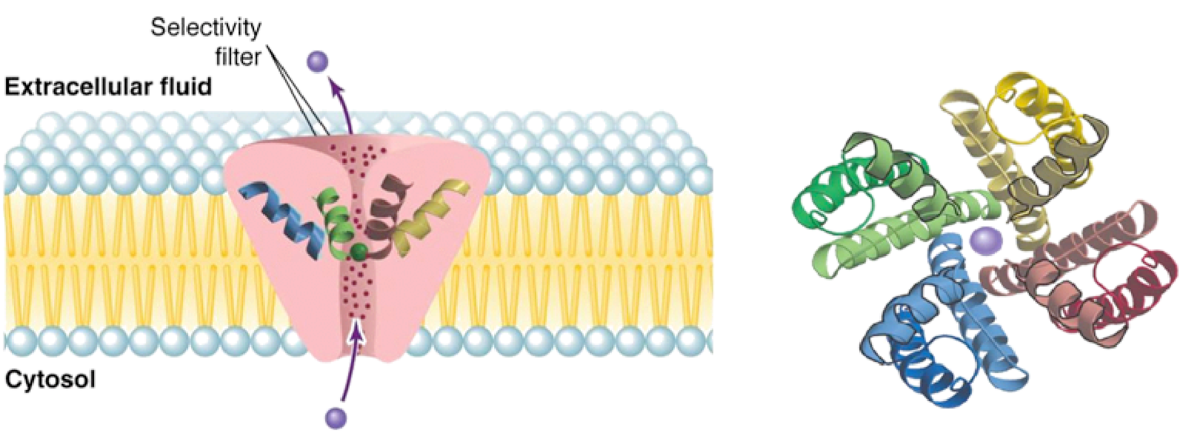

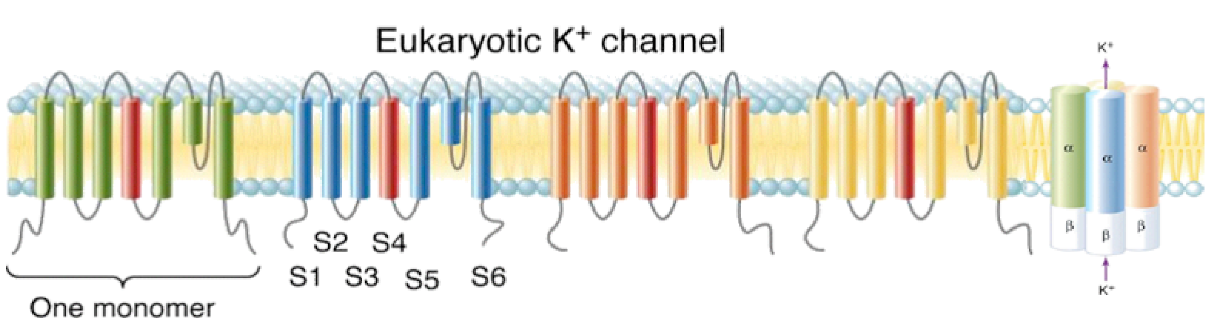

12_moleChannel.psd

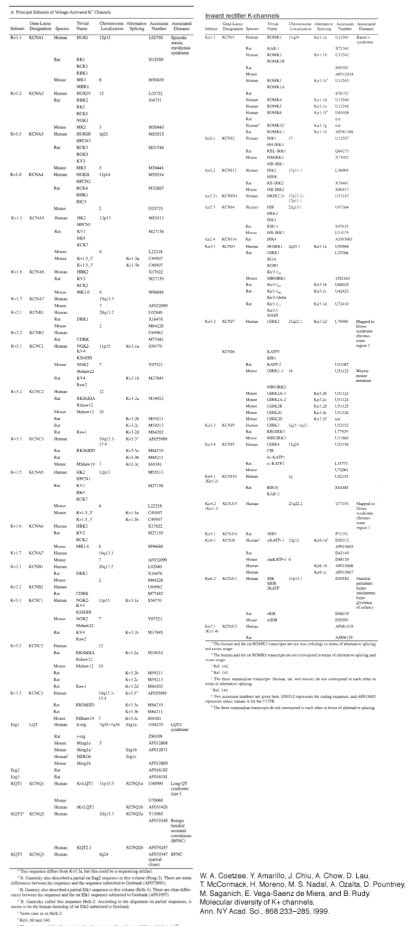

14_K_channels.psd

Hodgkin-Huxley Equation + a Zoo of Channels

injected current, leak current, sodium current, potassium current

$$C\frac{dV}{dt} = I_{stim} - g_L(V - V_L) - \bar{g}_{Na}m^3h(V - V_{Na}) - \bar{g}_K n^4(V - V_K)$$

persistent sodium current, transient potassium current (A-current)

$$-\bar{g}_{NaP}p^4(V - V_{NaP}) - \bar{g}_A a^4 b(V - V_A)$$

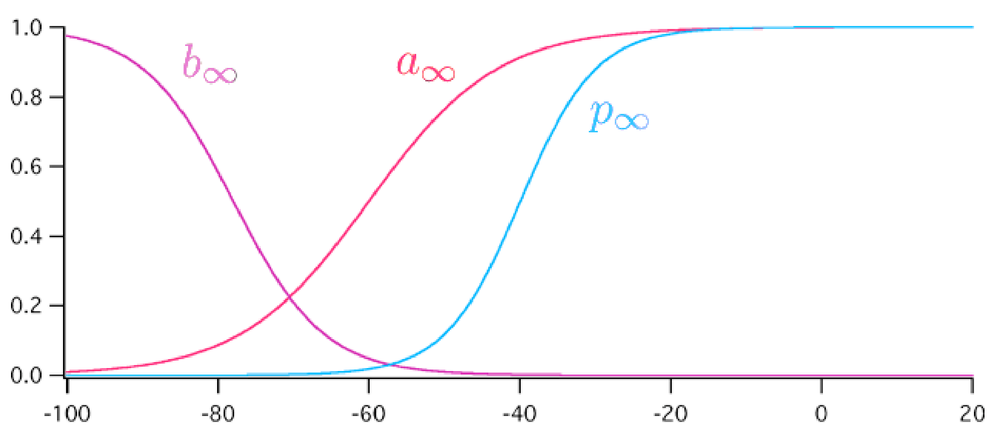

15_hh_plus.psd

Calcium is a Primary Intracellular Messenger

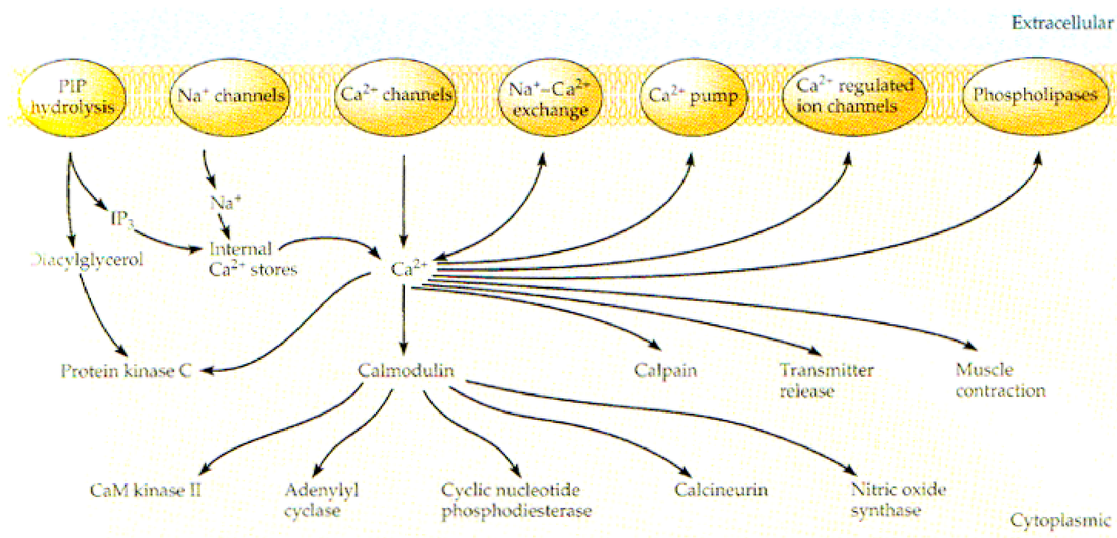

21_CaCells.psd

Calcium is Highly Buffered in the Cytoplasm

$[Ca^{2+}]_o = 2 - 5mM$

$[Ca^{2+}]_i = 10 - 100nM$

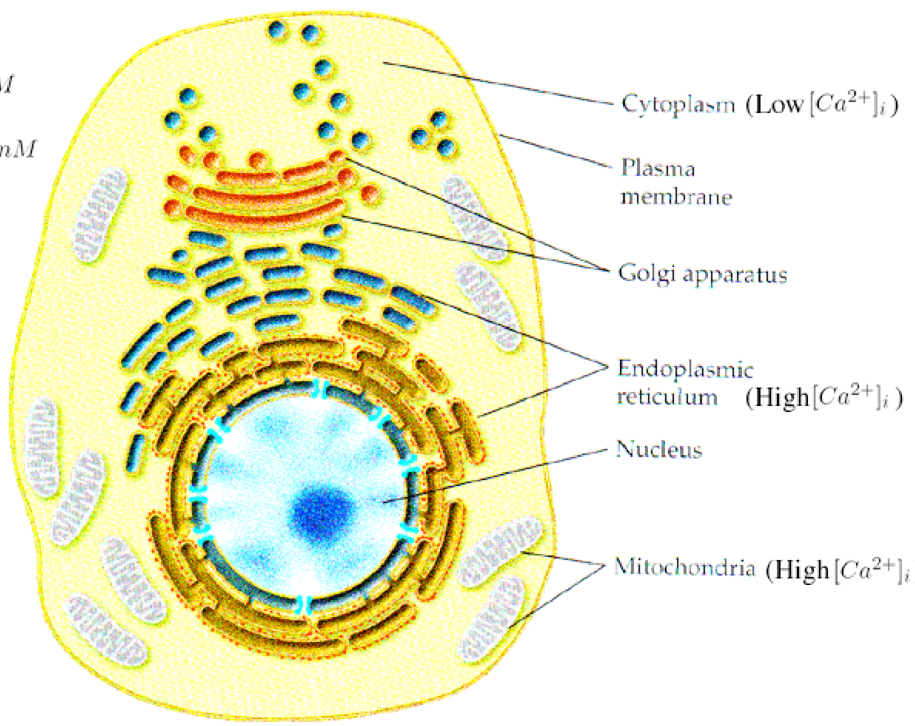

Linear model of removal and buffering:

$$\frac{[Ca^{2+}]_i}{dt} = \frac{1}{\tau_{Ca}}([Ca^{2+}]_\infty - [Ca^{2+}]_i)$$

22_buffered.psd

Goldman-Hodgkin-Katz Current Equation

$$I_{Ca} \quad = \quad P_{Ca} 2vF \frac{[Ca^{2+}]_i - [Ca^{2+}]_o e^{-v}}{1 - e^{-v}}$$

Faraday's const.
gas const.
Permeability

$$v \quad = \quad 2VF/RT \qquad\qquad P_{Ca} \quad = \quad -\frac{\text{(flux density across unit area of membrane)}}{\triangle[Ca^{2+}]}$$

Nernst Potential for Ca^{2+} (~140 mV)

$$E_{Ca} = 12.5 \cdot \log \frac{[Ca^{2+}]_o}{[Ca^{2+}]_i} \Rightarrow I_{Ca} \propto (V - E_{Ca})$$

23_Nernst.psd

High-threshold (long-lasting) Calcium Current

$$I_L = \bar{g}_L M^3 (V - E_{Ca})$$

High threshold Ca2+ current
-> allows calcium entry during action potential.

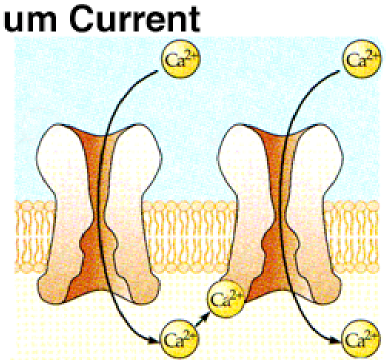

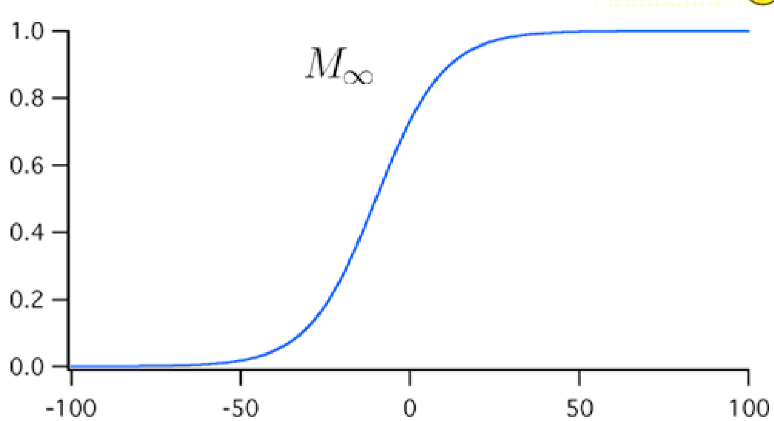

I_L is only activated at very depolarized levels.
Inactivation may depend on the intracellular Ca concentration.

24_iL.psd

Low-threshold (transient) Calcium Current

$$I_T = \bar{g}_T r^3 s(V - E_{Ca})$$

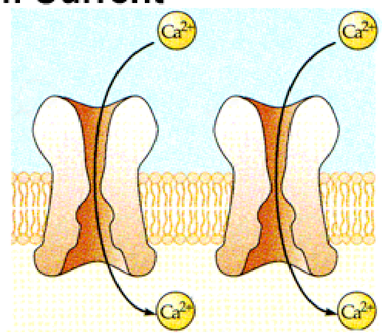

Transient low threshold Ca2+ current
-> generates a burst of action potentials.

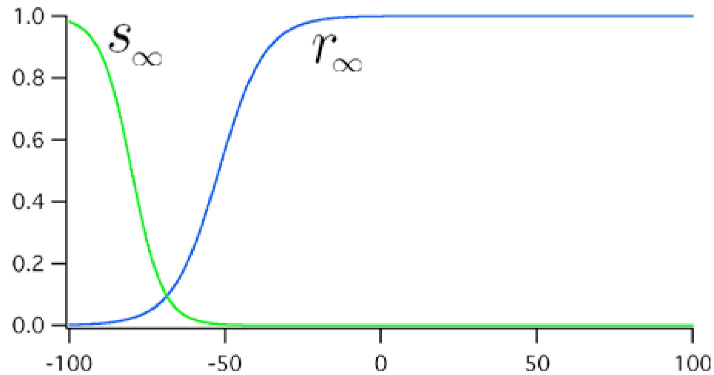

I_T is activated at lower voltages than the L current. Under physiological conditions the T current can be triggered by hyperpolarizing the membrane potential, which completly removes inactivation. A subsequent synaptic input activates a broad action potential, on top of which sodium spikes can ride.

25_iT.psd

Postinhibitory Rebound and Bursting

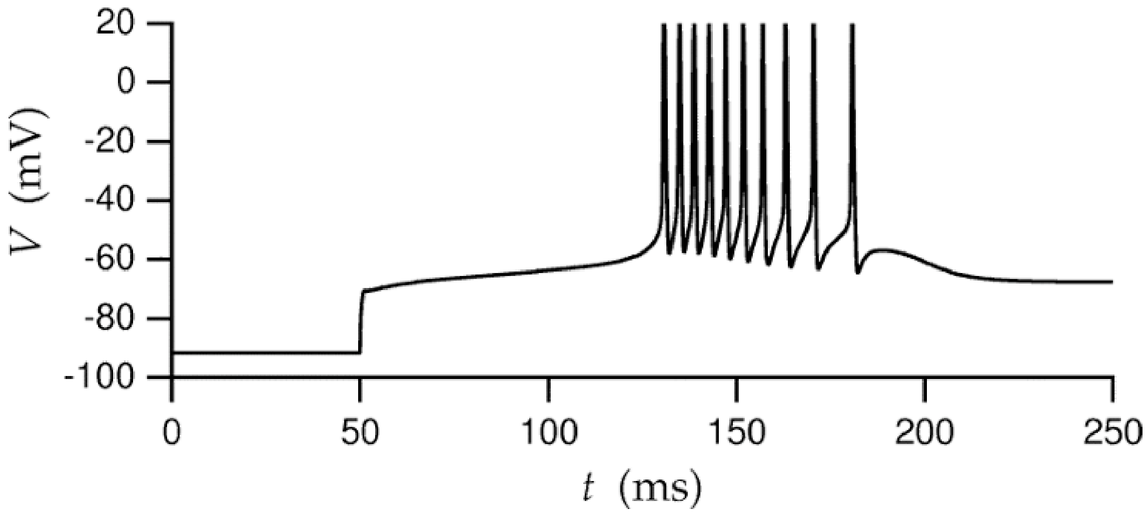

The model neuron was held hyperpolarized for an extended period (until the conductances came to equilibrium) by injection of constant negative electrode current. At t =50 ms, the electrode current was set to zero, and a burst of Na spikes was generated due to an underlying Ca2+ spike caused by a transient Ca2+ conductance. The delay in the firing is caused by the presence of the A-current in the model.

26_PIR.psd

Calcium-activated Potassium Current

$$I_C = \bar{g}_C n(V, [Ca^{2+}]_i)(V - E_K)$$

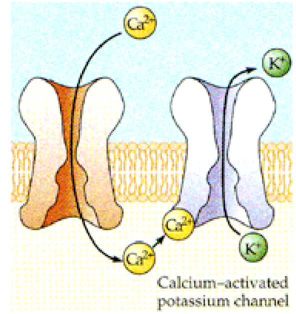

Ca^{2+} activated K^+ current
-> calcium and voltage dependent
-> involved in repolarization of action potential.

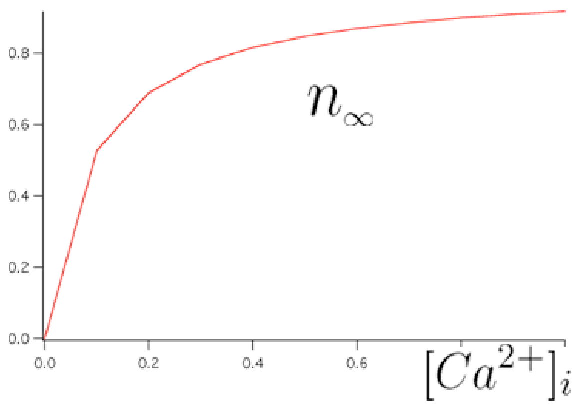

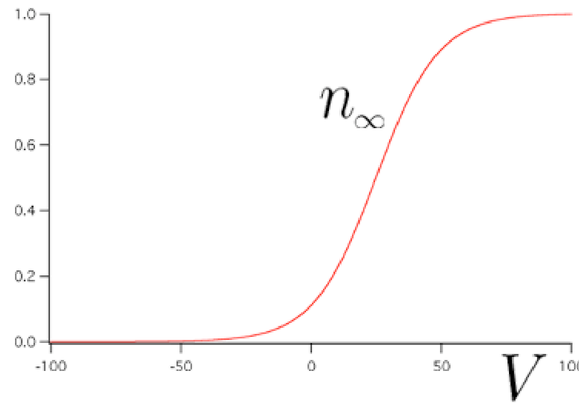

27_iC.psd

After-hyperpolarization Potassium Current

$$I_{AHP} = \bar{g}_{AHP} n([Ca^{2+}]_i)(V - E_K)$$

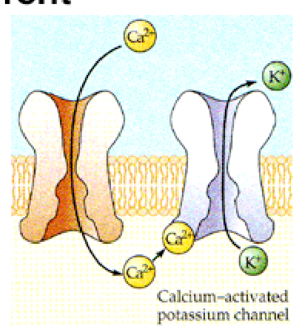

Slow, Ca2+ activated K+ current
-> calcium dependent, voltage independent
-> hyperpolarizes the cell after a spike train
-> slows down rate of action potential generation.

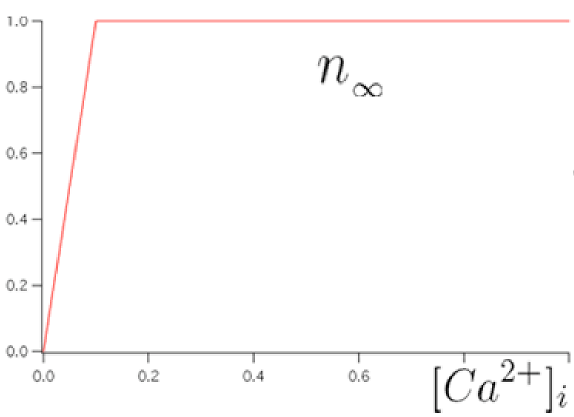

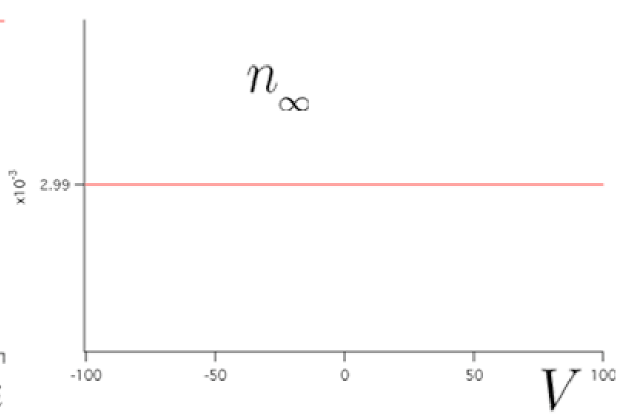

28_iAHP.psd

Interactions of Currents Generate Many Spike Patterns

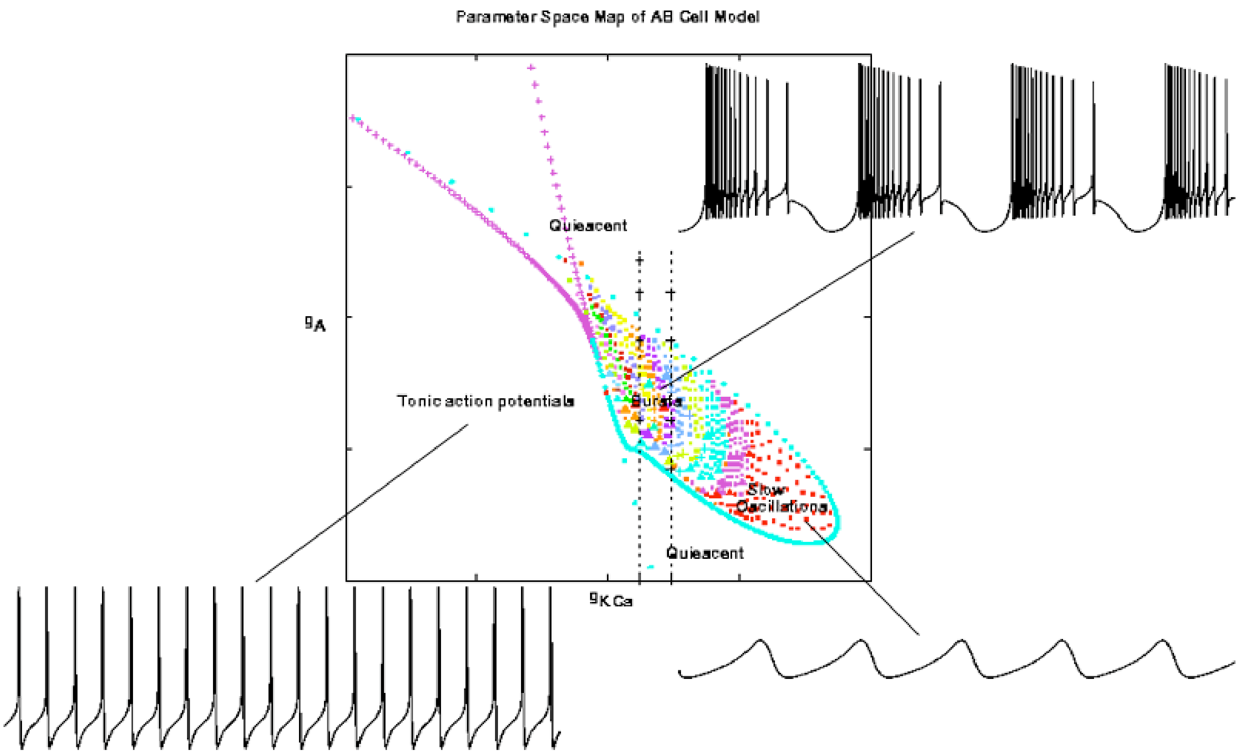

29_Guckenheimer.psd

The Same Spike Pattern may be Generated by Different Combinations of Current Densities

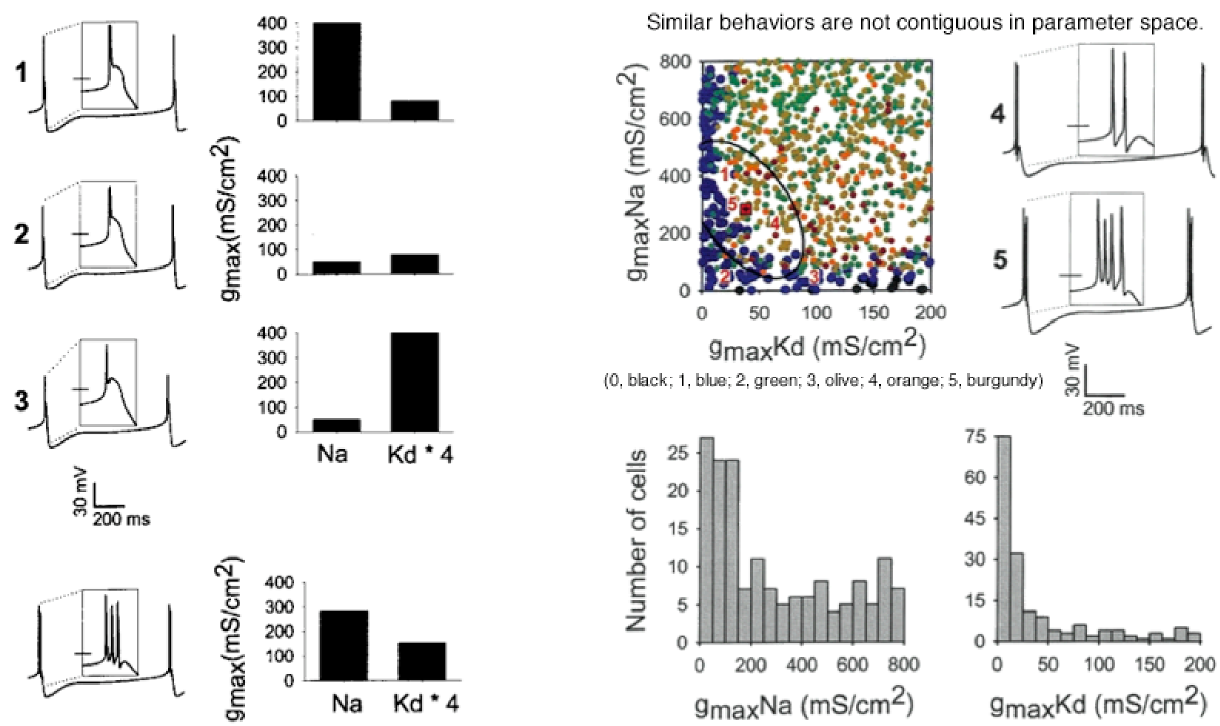

Failure of averaging in a conductance-based model.

Golowasch, Goldman, Abbott and Marder (2002)

30_Golowasch02.psd

The Same Spike Pattern may be Generated by Different Combinations of Current Densities

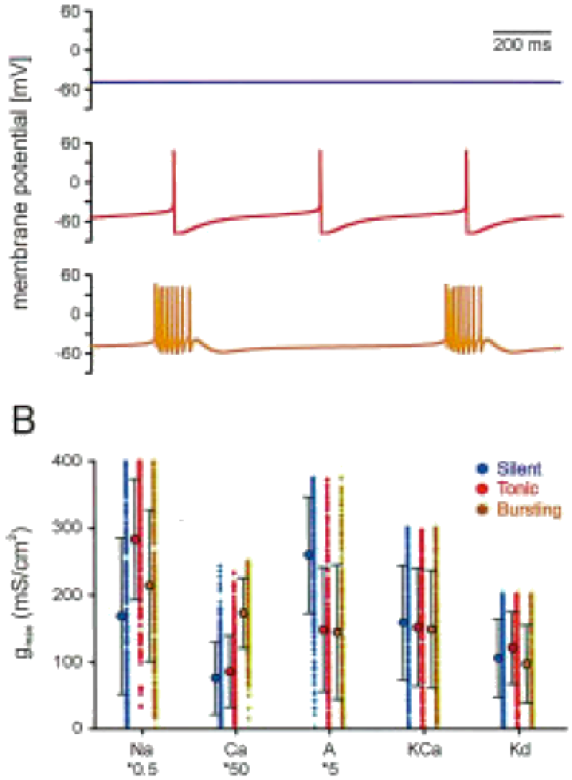

Marder and Prinz (2002)

31_Marder02b.psd

Combinations of Current Densities are Selected by Adaptive Processes in each Neuron Type

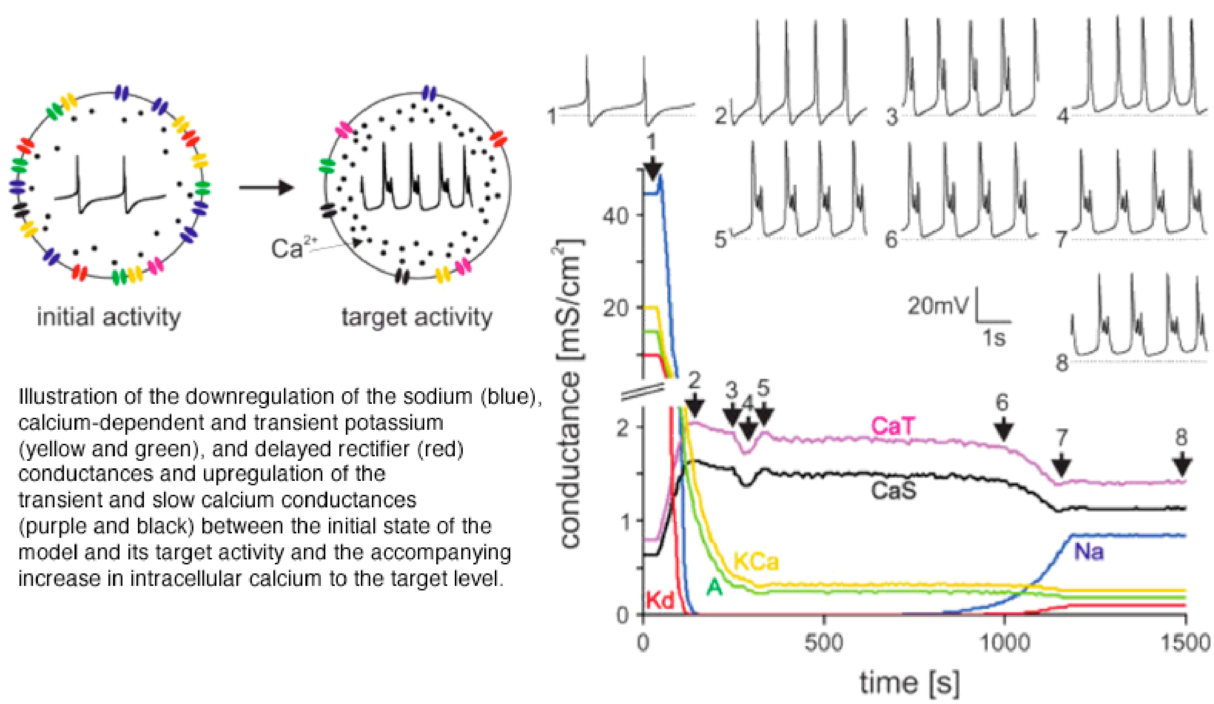

Illustration of the downregulation of the sodium (blue), calcium-dependent and transient potassium (yellow and green), and delayed rectifier (red) conductances and upregulation of the transient and slow calcium conductances (purple and black) between the initial state of the model and its target activity and the accompanying increase in intracellular calcium to the target level.

Marder and Prinz (2002)

32_Marder02b.psd